Radio Science, Volume 32, Number 2, Pages 579–591, March–April 1997

Effects of artificially modified ionospheres on HF propagation: Negative Ion Cation Release Experiment 2 and CRRES Coqui experiments

T. Joseph Fitzgerald, Paul E. Argo, and Robert C. Carlos

Los Alamos National Laboratory, Los Alamos, New Mexico

Abstract. We report the results of measurements obtained in conjunction with a series of high-altitude chemical release experiments of effects of artificially modified ionospheres upon high-frequency, ionospherically reflected radio paths. Computer simulations indicate that under optimum conditions, ionospheric modifications induced by chemical releases could perturb or even disrupt a communication channel; our experiments corroborate this but also indicate that it is very difficult to actualize such disruptions. Our experiments have shown that an ionospheric depletion, in which the electron density hole forms a huge radio frequency lens, generates new modes which, however, do not significantly affect a communications system. Under optimum path geometry a signal strength decrease of 10 dB or more is possible for several tens of minutes. Enhancements, such as those produced by barium releases, act as reflecting mirrors that can create a large shadow zone on the ground and block off significant amounts of energy. We measured signal strength decreases of up to 20 dB.

1. Introduction

In a previous paper we reported the results of an ionospheric modification experiment, the Nickel Carbonyl Release Experiment (NICARE 1), in which we investigated the effects of an electron density depletion on high-frequency (HF) propagation [*Argo et al.*, 1992; *Bernhardt et al.*, 1991]. *Mendillo and Forbes* [1982], *Bernhardt* [1987], *Mendillo* [1988], and *Bernhardt et al.* [1993] have modeled the electron density depletions produced by chemical releases in the ionosphere, but observations of effects on HF propagation are limited [*Booker*, 1961; *Kellogg*, 1964; *Chesnut et al.*, 1978; *Mendillo*, 1988]. Effects of electron density enhancements produced by the release of barium have been reported from a number of experiments [*Marmo et al.*, 1959; *Thome*, 1969; *Chang*, 1977]. Unlike these previous reports, our measurements during NICARE 1 were for a bistatic geometry similar to a HF communication path; the effects observed during NICARE 1 were well defined but weak [*Argo et al.*, 1992]. We detected the opening of new propagation modes, exhibited as weak (tens of decibels lower than the primary path) chirps in Doppler spectrograms. We report here on our measurements of the effects of electron density depletions and enhancements on oblique HF propagation obtained during the Negative Ion Cation Release Experiment 2 (NICARE 2) and Combined-Release and Radiation Effects Satellite (CRRES) Coqui chemical release experiments. We fielded a similar suite of experiments to the NICARE 1 campaign that were designed to quantify the HF propagation channel characteristics (Doppler fading rates, amplitude variations, etc.). We have also developed a computer simulation model which uses a three-dimensional ray-tracing program (TRACKER [*Argo et al.*, 1992]) to calculate the path of radio energy through an ionosphere modified using a simplified chemistry model derived from the work of *Bernhardt* [1987]. Our computer simulations indicate that under optimum conditions we would be able to detect strong effects of depletions or enhancements on the propagation channel. In particular, new modes would be generated and existing modes would undergo Doppler shifts and large-amplitude changes. This paper discusses our measurements of phase path changes (Doppler), angle of arrival changes, and amplitude changes for the two sets of experiments.

Our experiments employ long-path, one-hop HF propagation using primarily continuous wave (CW) signals

Paper number 96RS03597.
0048-6604/97/96RS-03597$11.00

spaced in frequency and multiple receiver antennas to detect spatial effects. In the NICARE 1 experiment we had two propagation paths that crossed at the expected chemical release point from almost perpendicular directions [*Argo et al.*, 1992]. For the experiments reported here, which occurred in different geographic locations, we employed different path geometries. The first experiment, called NICARE 2, consisted of the release of barium and sulfur hexaflouride at two separate locations along the same magnetic field line; the chemicals were released from a rocket launched from Kwajalein Atoll, Marshall Islands. We used only one propagation path that intersected the midpoint between the releases. The second experiment, CRRES Coqui, was a series of barium enhancements and a single depletion. The rockets were launched from Puerto Rico. We fielded four closely spaced paths with tens of kilometer separations between the two transmitter sites and about 100 km between the two receiving sites. This was done in order to understand the larger-scale variations in propagation that might be exhibited during the ionospheric modification. In addition, we deployed receiver antenna arrays with dimensions of almost a kilometer to measure smaller-scale variations.

2. Experimental Setups

In our experiments we observed the effect of the ionospheric modifications remotely using oblique HF sounders which were deployed so that the HF reflected in the ionosphere near the nominal release locations.

2.1. NICARE 2

The NICARE 2 experiment consisted of the release of barium and sulfur hexaflouride at two separate locations along the same magnetic field line to observe chemical and plasma interactions between the enhanced ionization created by the Ba and the depletion created by the SF_6 [*Bernhardt et al.*, 1993]. The separation was achieved by releasing the Ba on the upleg and the SF_6 on the downleg of a rocket launched from the Kwajalein Missile Range in the equatorial Pacific on August 22, 1990. The releases were at the same altitude (380 km) in the postsunset (0816 UT launch) *F* region. We observed the effects of the ionospheric modification by deploying CW and pulse oblique HF sounders over a 700 km path between Maloelap Atoll and Bikini Atoll so that the great circle connecting the transmitters and receivers nearly bisected the intended locations of the releases. The transmitters were located at Maloelap Atoll (8.70° N, 171.23° E) as shown on the map in Figure 1. The receivers were located at Bikini Atoll (11.63° N, 165.54° E), giving a ground range of 702 km. The great circle connecting the transmitters and receivers bisected the locations of the releases (SF_6, 10.75° N, 168.05° E; Ba, 10.25° N, 167.85° E). Because of a difference between the planned and achieved

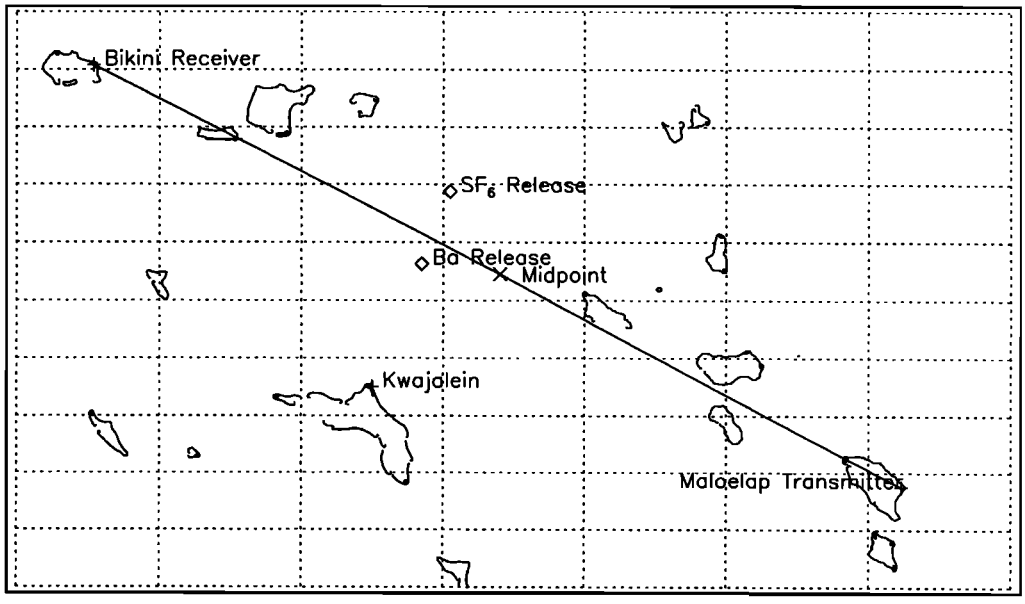

Figure 1. The location of the Ba and SF_6 releases in relation to the great circle paths between transmitters at Maloelap Atoll and receivers at Bikini Atoll for the Negative Ion Cation Release Experiment 2 (NICARE 2).

trajectories, the Ba was released close to or below the solar UV terminator, and thus the expected ionization was inhibited; reconstruction of ionospheric densities using beacon transmissions from the payload indicate that the expansion of the neutral Ba created a momentary depletion [*Bernhardt et al.*, 1993]. The beacon measurements also indicated that the SF_6 created a large electron density depletion; an enhancement attributed to photoionization of the Ba was also observed [*Bernhardt et al.*, 1993]. Changes in the spectra and group delay of our HF signals indicate that the SF_6 created a large electron density depletion and induced a lens-like refraction perturbation on the HF signals.

In this experiment we employed two types of sounders: the CW Doppler and a channel probe. The former consisted of four CW transmissions with the lowest frequency at 10.224 MHz and other frequencies offset higher by 0.5, 1.5, and 4.0 kHz. The CW tones were generated by four frequency synthesizers which were locked to the 10 MHz output of a rubidium oscillator. The outputs of the synthesizers were fed into four linear amplifiers. The amplified CW was combined in two pairs and fed into two antennas. The lower two frequencies fed a delta antenna tipped at an angle of 45° toward the receiver, while the upper two frequencies fed an end-fired delta antenna with its plane parallel to the nominal great circle path. The antennas were supported by the same mast (15.2 m high); the base legs were 30.4 m long, while the side legs were 21.3 m long. The power output at each frequency was 50 W; the gain of the tilted delta along the nominal ray path was 1 dB while that of the end-fired delta was –9 dB. Antenna modeling shows that the radiation from the tilted delta should have been horizontally polarized while that from the end-fired delta should have been vertically polarized. Our data suggest, however, that for an unknown reason the radiation from the tilted delta had an intermediate polarization between vertical and horizontal. Magnetic loops of 1 m diameter were used as the receive antennas for the CW transmissions; the planes of the loops were aligned parallel to the plane of the ray path. The bottoms of the loops were supported approximately 6 cm above the ground.

The CW transmissions were detected using either Collins S1 or Racal 6790 receivers operated in CW mode at a beat frequency of 200 Hz with a bandwidth of 200 Hz. The frequency of the receivers was locked to an external rubidium clock. An array of eight such systems were deployed in a "T" pattern, with six elements normal to the ray path and three elements parallel to the ray path as shown in Figure 2. The antenna separations varied

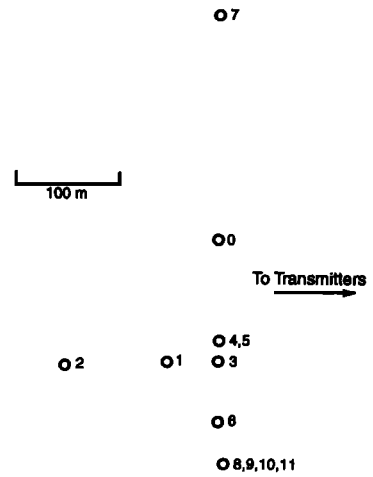

Figure 2. Plan view of the locations of the eight antennas used for the CW spatial array in the NICARE 2 experiment. Numbers indicate the receiver channels.

from a minimum of 25 to 450 m in the transverse direction and 50 to 150 m along the path. The receivers were operated without automatic gain control; the audio output of each receiver was digitized at a rate of 600 Hz. A receiver connected to each of the eight antennas monitored the transmission at the base frequency; an additional three receivers connected to one antenna monitored the transmissions at the upper three frequencies. This CW Doppler system was essentially the same as that used for the NICARE 1 experiment [*Argo et al.*, 1992].

The transmission for the channel probe consisted of a phase-coded pseudorandom sequence with a bandwidth of 60 kHz at a nominal frequency of 10.6 MHz. The sequences had a chip length (duration of element of the sequence) of 16 μs, a length of 256 chips, and a repetition rate of 20 Hz. The timing was controlled with the 10 MHz output of a Global Positioning System (GPS) receiver. The output power was 500 W from a separate tilted-delta antenna. The channel probe transmissions were detected with a tilted-delta antenna which fed a 2 MHz bandwidth receiver. The output of the receiver at an intermediate frequency of 1 MHz was fed into a mixing circuit which formed the inphase and quadrature components, beat the signal down to base band, and low-pass filtered the result with a total bandwidth of 60 kHz. The resulting two channels of data were digitized at a rate of 120 kHz for periods of 8 ms centered on the transmitted sequence. The timing of the transmitter and receiver was controlled by a GPS receiver. The digitized data were stored on magnetic disk.

2.2. CRRES Coqui

The CRRES Coqui (hereinafter referred to as Coqui) campaign of sounding rocket chemical releases undertaken during the summer of 1992 consisted of five barium enhancement releases and one trifloromethyl bromide depletion release. The rockets were launched from a site near Vega Baja, Puerto Rico, during two moon-down periods [*Djuth*, 1993]. During the first period (May 25-June 6) a small dusk Ba release, a postmidnight depletion release, and a small dawn Ba release were undertaken. During the second campaign period (July 2-July 12), three large dawn Ba releases were conducted. We operated HF propagation paths during five of the six release experiments as follows: for the first Ba release and the CF_3Br depletion release during the first period and for the three barium releases of the second campaign period. The first experiment of the Coqui campaign, rocket AA3a, was launched on May 25, 1992, at 2348 UT; it released two 1.1 kg canisters of Ba at altitudes of 251 and 271 km. The second rocket, AA4, released nearly 30 kg of CF_3Br at 0813:49.3 UT, a few hours before sunrise, on May 30, 1992, at a geographic location of 18.97°N, 66.60°W and 283 km altitude [*Bernhardt et al.*, 1995]. The three large barium releases were nominally similar; all were predawn releases at approximately 250 km altitude (on the bottomside of the *F* layer). The AA1 rocket, which was launched on July 2, released 22 kg of Ba at 0903:33 UT at 255 km altitude and coordinates 18.82°N, 66.72°W. The AA7 rocket released 22 kg of Ba at 0900:21 UT on July 4 at 254 km altitude and at 18.91°N, 66.80°W. The last rocket, AA2, released 35 kg of Ba at 253 km altitude on July 12, 1992, at 904:32 UT and location 18.82°N, 66.64°W [*Djuth et al.*, 1995]. As a part of the Coqui campaign, there were detailed diagnostics set up around Arecibo, Puerto Rico; these included the incoherent scatter radar, optics, and a digital ionosonde at Ramey, Puerto Rico [*Djuth*, 1993].

We used four long bistatic propagation paths for the Coqui experiment (Figure 3). Unlike the NICARE 1 pair of paths, which were very different in geometry, the Coqui set of paths were designed to be nearly identical. This allowed us to investigate the local variations in effects from the chemical releases. The receive sites (which each observed two transmitter sites) were separated by about 100 km, while the transmit sites, which were located on Guadeloupe, were separated by approximately 40 km; the transmitter coordinates were 16.0°N, 61.75°W and 16.25°N, 61.5°W. The receiver sites were in the Turks and Caicos Islands at Providenciales (21.8°N, 72.3°W)

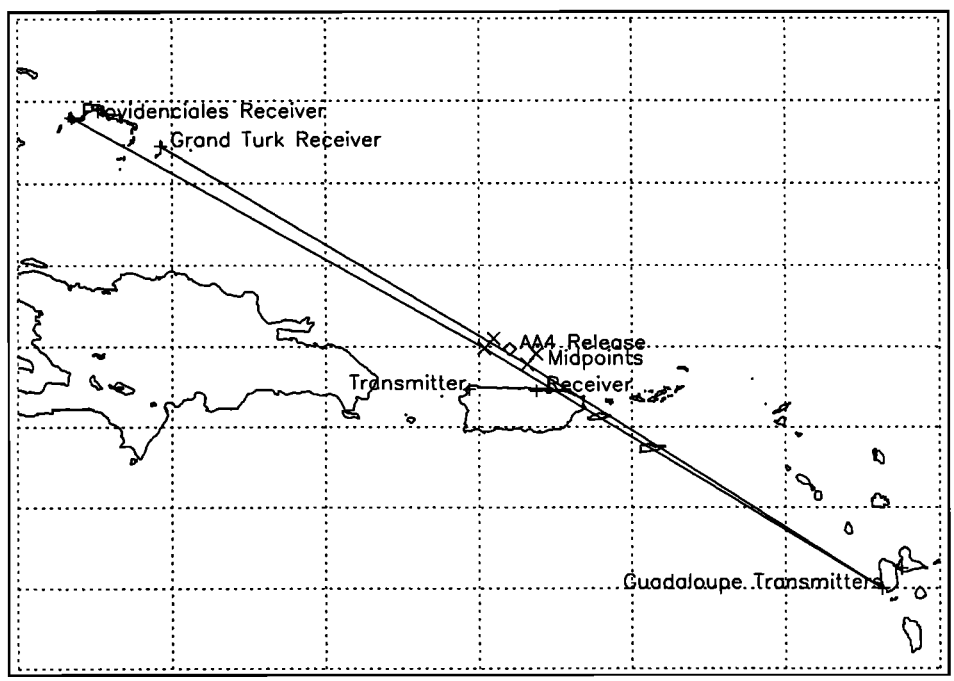

Figure 3. CRRES Coqui campaign setup, showing the four long bistatic propagation paths (two transmit sites on Guadeloupe and receiving arrays on Grand Turk and Providenciales) and a quasi-vertical path from Sabana Seca, Puerto Rico, to Ramey, Puerto Rico.

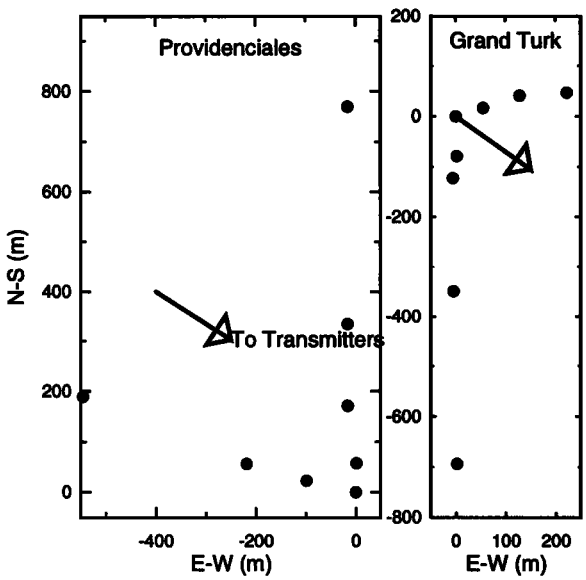

Figure 4. Plan view of the locations of the antennas used for the CW spatial arrays in the Coqui experiment for (left) Providenciales array and (right) Grand Turk array.

and Grand Turk (21.45°N, 71.15°W) . Both receive sites had a CW Doppler system, while one path also had a bistatic channel probe and oblique ionogram [*Wagner and Goldstein*, 1983]. In addition, we fielded a CW bistatic system on Puerto Rico with the transmit site at the Ramey (18.47°N, 67.13°W) and the receive site at the Sabana Seca near San Juan (18.45°N, 66.25°W). This system allowed us to study the effects of the chemical releases on "quasi-vertical incidence" propagation paths. Because the releases were about 50 km to the north of the nominal reflection point, this path was not optimally sited to observe the maximum effects.

The CW portion of the receiving sites employed a set of crossed antenna arrays with each antenna feeding a separate receiver and one antenna feeding each of four frequencies into separate receivers (Figure 4). Each site had 12 receivers. The array spacings, as in NICARE 1 and 2, varied by nearly 1 order of magnitude. Because we were at midlatitudes, we did not expect to have to contend with spread *F* effects that were observed during NICARE 2 campaign so we could employ larger array spacings ranging up to 750 m. The receive antennas were the

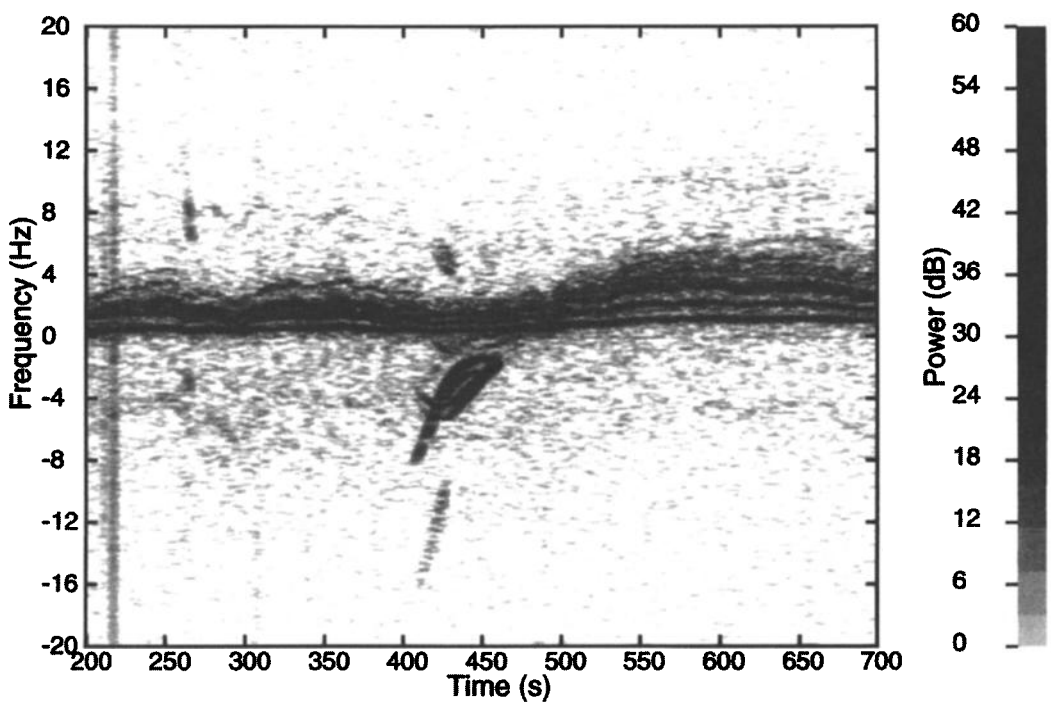

Figure 5. Doppler power spectra of one CW transmission frequency versus time after launch for the NICARE 2 experiment. The power is coded according to the gray scale at right. Note that the chirped signal never joins the main propagation mode.

same type used in the NICARE 2 measurements. The frequencies of the two transmitter sites were offset by 30 Hz so that one receiver could monitor both sites.

3. Results

3.1. Doppler Spectra

Because of time variations in the index of refraction of the ionosphere, the phase of a received CW signal will vary, resulting in a small Doppler shift of the transmission which depends on the exact ray path. Negative Doppler shifts correspond to increasing phase paths. Thus multipath propagation appears as multiple peaks in the power spectra with different frequency shifts for each component.

3.1.1. NICARE 2 Figure 5 shows the evolution of the Doppler spectra versus time after launch on one channel tuned to the base frequency. The ionosphere was unusually quiet on this night; on other nights, spread *F* occurred and greatly broadened the Doppler spectra. Also, the postsunset rise of the *F* layer had ended early, so that the Doppler shift was near zero. Additional peaks in the spectra toward positive Doppler were caused by multiple ionospheric reflections, each of which adds to the Doppler shift. There was an abrupt appearance of peaks at negative Doppler following the SF_6 release at 404 s; these peaks persisted for about 50 s. There was also some weaker structure near zero Doppler and at positive shifts at the same time. Some weak structure appeared at the time of the Ba release (273 s), probably associated with the momentary depletion caused by the expanding Ba.

If the spectrogram for the time period around the SF_6 release is examined in detail as shown in Figure 6, we notice that four peaks appeared. At 430 s there were peaks at –5, –4, –3, and –2.5 Hz. They started in two pairs; one pair at a Doppler shift of –8 Hz and the other pair at a shift of –3 Hz. The pair with the high Doppler shift moved to lower Doppler and separated, while the pair with low Doppler moved to higher Doppler before reversing and moving to lower Doppler. One peak of each pair joined together and disappeared; the first junction was at 450 s, while the second junction occurred approximately 10 s later. These junctions are reminiscent of the behavior of high and low rays at the approach to penetration in the normal ionosphere when the ambient electron density decreases. We attribute the appearance of peaks in pairs to polarization splitting; that is, the *o* and *x* modes had phase path changes which were slightly different so that they appeared as separate peaks in the Doppler spectrogram.

In Figure 6 we compare the Doppler spectra from the following two different antennas: the first is that from a receiver tuned to the base frequency broadcasting a wave that excited both polarizations; the second is from a receiver tuned to the transmission from the vertically polarized antenna at 1.5 kHz above the base frequency. Comparing the relative power in the peaks at –1.7 and –2.4 Hz in the two spectra at 440 s, we note a difference of 4 dB in the first versus a difference of 14 dB in the second. This indicates that the vertically polarized antenna, which should mainly have excited the *x* mode, generated a 10 dB difference in the power of the two modes. It is unlikely that the small frequency difference would make a significant difference in the propagation. The spectra for the other frequency (+4 kHz) broadcast from the vertically polarized antenna also showed a similar enhancement. We estimate that the angle between the wave vector and the magnetic field at the point at which the ray entered the ionosphere was 89°, assuming a dip of 12°, a declination of 8.5°, and a virtual reflection height of 500 km.

3.1.2. Coqui We spaced the transmission frequencies following the AA4 depletion release between 8 and 11 MHz in 1 MHz steps. All paths observed effects; the most significant effects were observed at the higher frequencies. We believe that the lower frequencies were propagating at a significantly lower altitude than the release height and were affected only later in the development of the disturbance. The quasi-vertical path observed a set of new modes with a Doppler width of almost 4 Hz. However, the signal strengths in these spread modes were down by nearly 10 dB from the primary mode. The oblique paths exhibited more effects than we had seen on the NICARE 1 and 2 experiments, with a maximum signal strength change of nearly 10 dB. At least a small Doppler shift occurred on most frequencies for all paths. Figure 7 shows the Doppler spectrograms for the lowest (8 MHz) and highest (11 MHz) frequencies. The 11 MHz data show modes with large negative Doppler formed at release time similar to the observations for NICARE 1 [*Argo et al.*, 1992]. It also showed a mode with large positive Doppler at release time which may be associated with the expansion of the chemical vapor; a weak mode with positive Doppler appeared at the time of release for NICARE 2 (Figure 5). At 11 MHz the new mode with large initial negative Doppler persisted as a peak near zero Doppler by 400 s after launch; at that time the preexisting ray path had been perturbed to a Doppler shift of about –1 Hz. The lowest frequency showed only a similar perturbation to the preexisting ray path. Effects at the highest frequency persisted for least 500 s.

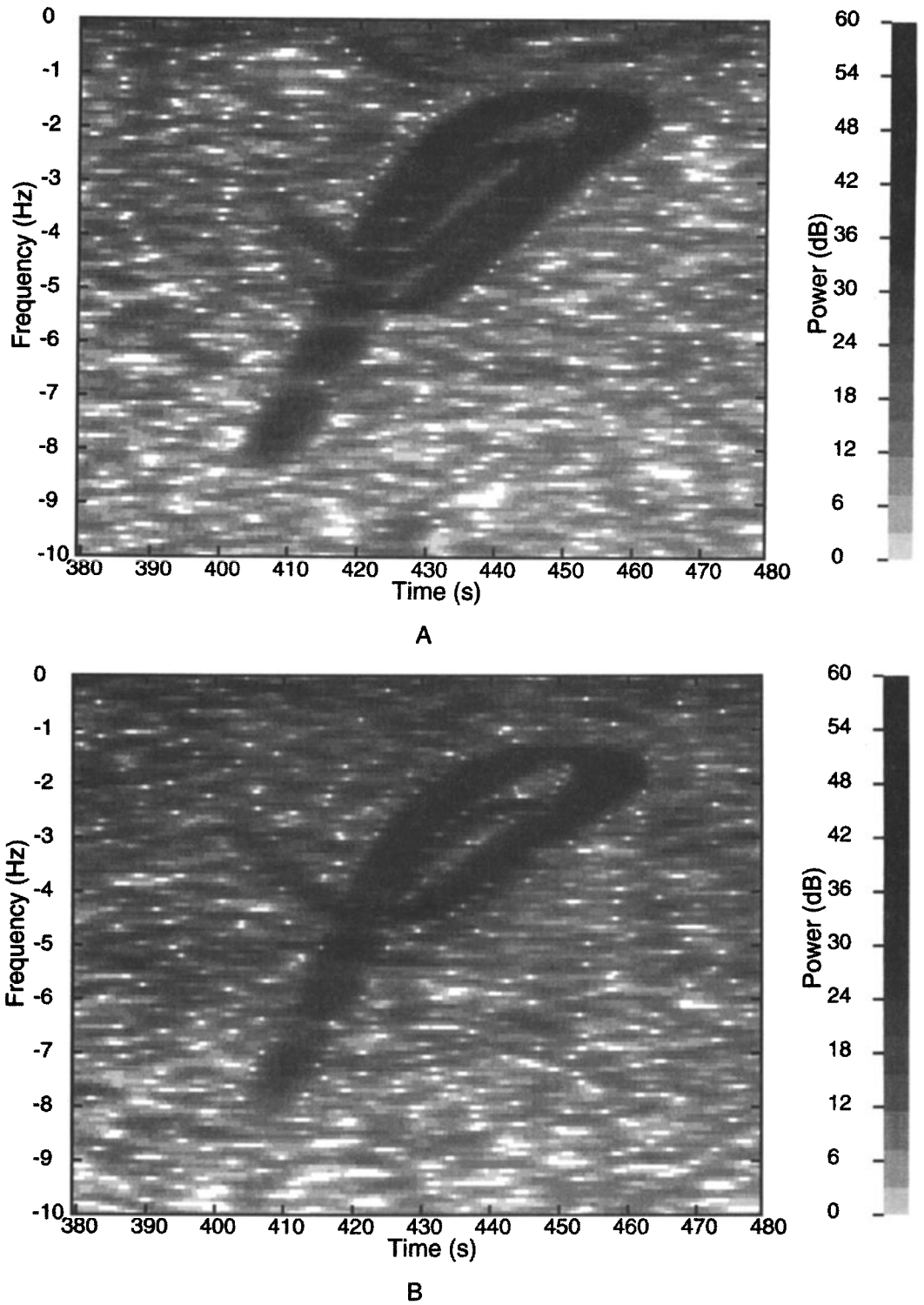

Figure 6. (a) Detail of the Doppler spectrogram of the CW frequency from Figure 5 showing the simultaneous occurrence of four Doppler-shifted modes. The appearance of almost duplicate traces is believed to be the ordinary and extraordinary polarization modes. (b) The signal from a different transmitting antenna, with a different polarization, which shows the suppression of one of the magnetoionic modes.

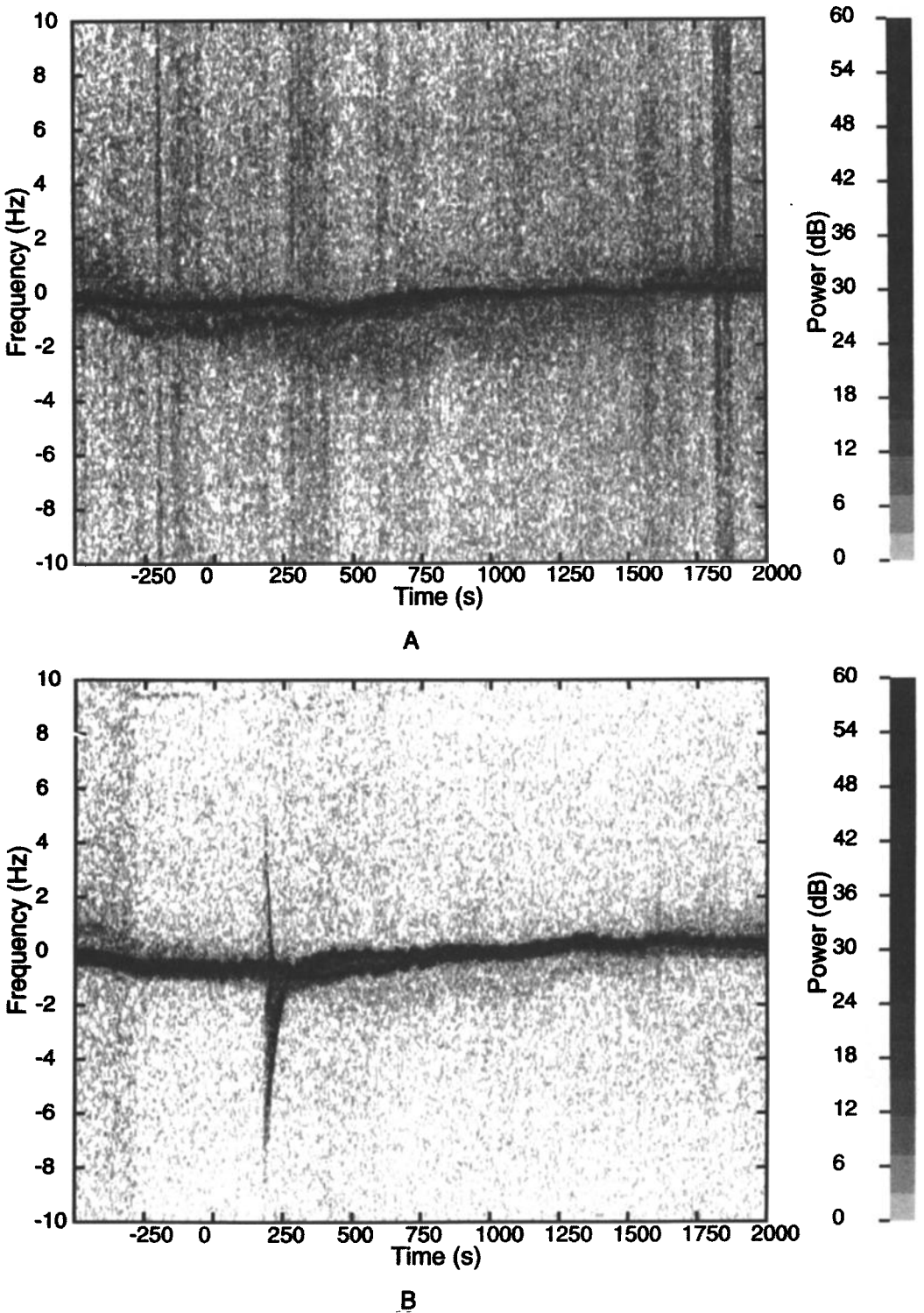

Figure 7. Doppler power spectra versus time after launch from the Coqui depletion experiment (AA4) for two frequencies on the South Guadeloupe to Providenciales path at (a) 8 MHz and (b) 11 MHz. Release occurred at 170 s after launch. Note that although both paths had the primary propagation mode affected, only the higher frequency had extra depletion modes supported.

The Doppler spectrogram, Figure 8, for the path from the southern transmitter on Guadeloupe to Grand Turk following the AA3a Ba release experiment showed chirps at the time of the two barium releases. These chirps were observed on a wide range of transmission frequencies, from 10 MHz to 14 MHz. The northern Guadeloupe to Grand Turk path was not affected. The quasi-vertical path on Puerto Rico also observed both releases as weak chirps. Chirps with predominantly negative Doppler shift were observed at release time for the NICARE 1 depletion release [*Argo et al.*, 1992] and for the NICARE 2 and AA4 depletion experiments reported here. Negative Doppler shifts produced by depletions mean that the phase path was increasing and indicate that the ray was refracted around the edge of the expanding depletion. On the other hand, chirps with positive Doppler shifts such as those seen in Figure 8 are indicative of a reflection from an expanding ion cloud which is off the great circle path. With time, the development of the ionospheric modification slows down and the Doppler shift decreases to zero.

Figure 9 shows the Doppler spectrogram for the North Guadeloupe to Providenciales path at 7.3 MHz for the first large barium release (AA1). The two Doppler peaks existing before the launch were probably *o* and *x* modes; notice that they suddenly decreased in signal strength by at least 30 dB at about 400 s and remained perturbed for over 30 min. Figure 10 shows the effects of the third large barium release (AA2) on the same path but at a frequency of 9.3 MHz. These data show some of the complications in understanding the effects of the release. There were multiple propagation modes caused by multihop during the sunrise transition. The primary one-hop mode was centered near 0 Hz, while the modes at positive Doppler were multihop paths. Notice that the single-hop mode decreased in power by nearly 20 dB for 15 min or longer.

3.2. Angle of Arrival Measurements

NICARE 2 To clarify the effects of the ionospheric modifications, we have examined the angle of the modes generated by the NICARE 2 depletion. As with the NICARE 1 experiment, data from the spaced antenna array in NICARE 2 could be used to estimate the angle of arrival of any new modes relative to the undisturbed propagation. We calculate the angle of arrival using a delay-and-sum beam former algorithm and Doppler filtering to

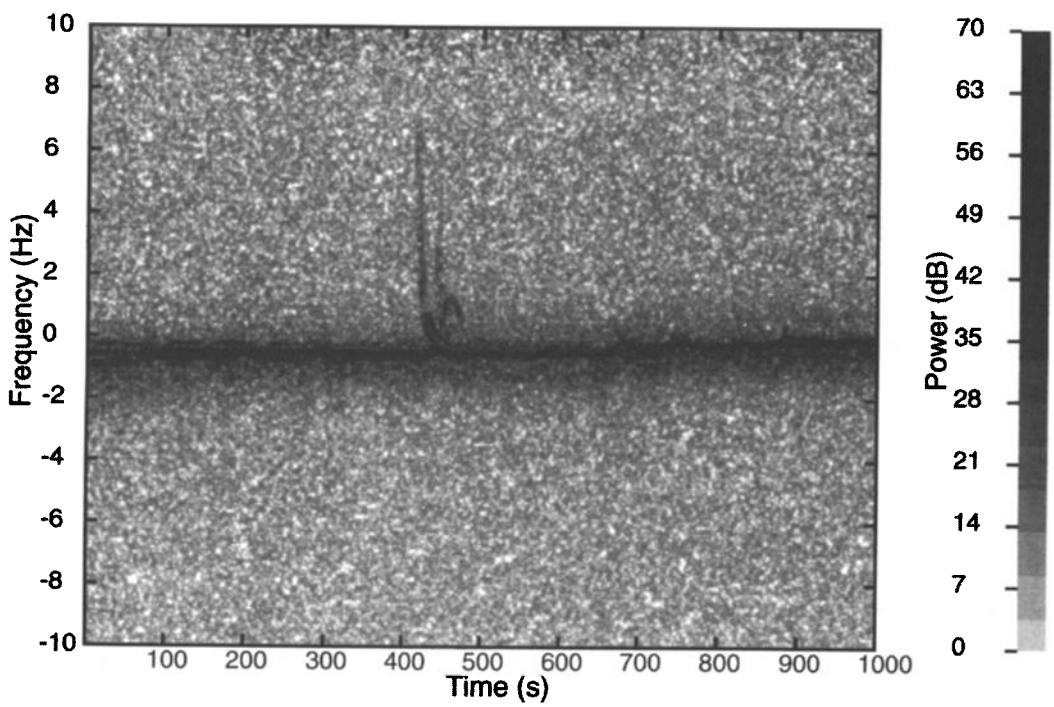

Figure 8. The Doppler spectrogram versus time after launch for the series of Coqui small barium releases (AA3a) for one of the oblique paths that also showed an effect; note the pair of weak chirps corresponding to the release times (410 and 436 s).

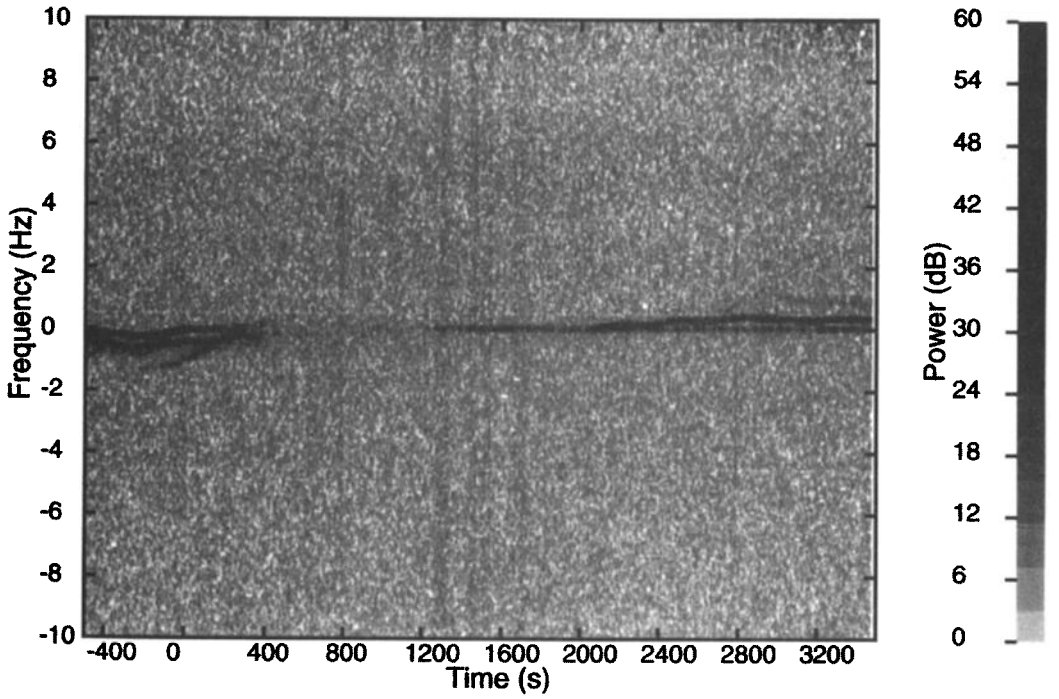

Figure 9. Doppler spectra versus time after launch for a large barium release (AA1) for the transmission between Guadeloupe and Providenciales at 7.3 MHz. It shoes a greater than 30 dB signal strength decrease after the formation of the barium ion cloud. Release was at 141 s.

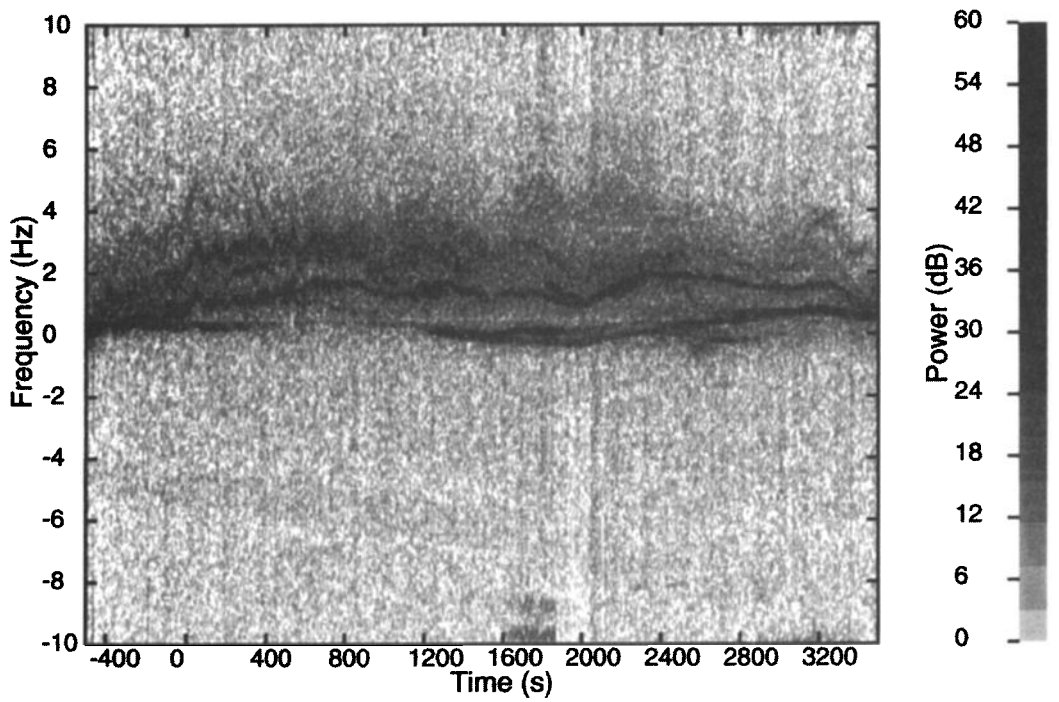

Figure 10. Doppler power spectra versus time after launch for the third large barium release (AA2) at a frequency of 9.3 MHz showing the presence of multihop propagation. Release occurred at 152 s. Signal strength on the one-hop mode near 0 Hz decreased by more than 20 dB for more than 800 s.

separate the multipath components [*Argo et al.*, 1992]. The results are shown in Figure 11, where we plot the elevation angle and the azimuth (clockwise relative to the undisturbed one-hop ray) between 405 and 455 s after launch for the Doppler shifts showing enhanced power. We identify the following two components in the Doppler spectra (Figure 6): the first, which we call the large initial Doppler component, started with a shift of –8 Hz and decreased to a shift of –2 Hz; the second, which we call the small initial Doppler component, started with a shift of –3 Hz, attained a maximum shift of –4.5 Hz, and finally merged with the first component. Initially, the rays were at approximately the same elevation angle as the undisturbed ray but were displaced to the north. Both components started off at approximately the same angles of arrival; with time, the component with large initial Doppler was displaced farther to the north and to a lower elevation angle. There is more scatter in the data for the small initial Doppler component, but it appears that, with time, it was displaced to the north and initially to higher elevation angle. We could not track the angle of arrival of this component for the full duration of the perturbation, but it is likely that it eventually moved to the direction of the large initial Doppler component before the extinction of the perturbation. From these measurements it appears that the depletion refracted the ray paths around its northern edge; that edge progressed rapidly northward until finally, the refractive power of the lens-like perturbation was no longer able to bend the rays to our receiver and the rays were extinguished.

3.3. Signal Strength Changes

No change in amplitude to the main one-hop propagation mode was observed during the NICARE 2 experiment because the depletion was well away from the great circle path. The Coqui releases were closer to the nominal one-hop ray paths and did show amplitude effects.

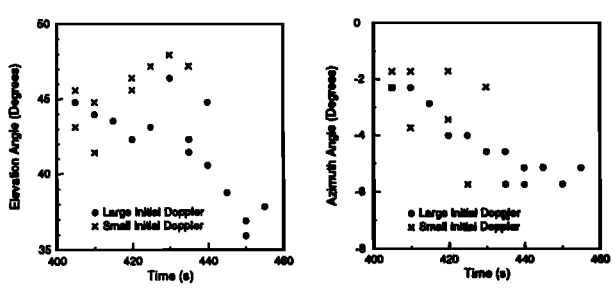

Figure 11. Direction of arrival of secondary signal produced by NICARE 2 depletion shown as a function of time.

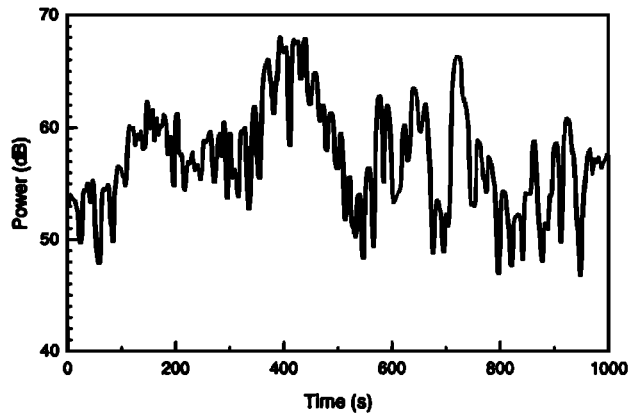

Figure 12. Total received power versus time after launch of the AA3a rocket for the South Guadeloupe to Grand Turk path at 11.33 MHz. The two small barium releases at 410 and 436 s produced no observable effect compared to the preexisting fluctuation level.

The first barium released, AA3a, did not produce significant changes in the total received amplitude (Figure 12). There were amplitude fluctuations in the data but none that can unequivocally be connected to the barium releases. The second large barium release (AA7) showed a 10 dB signal fade immediately after the release on all four paths at the higher frequencies. The southern Guadeloupe transmitter to Providenciales path showed a 10 dB dropout that was sustained for nearly an hour (Figure 13). The other paths and frequencies recovered within a few tens of minutes.

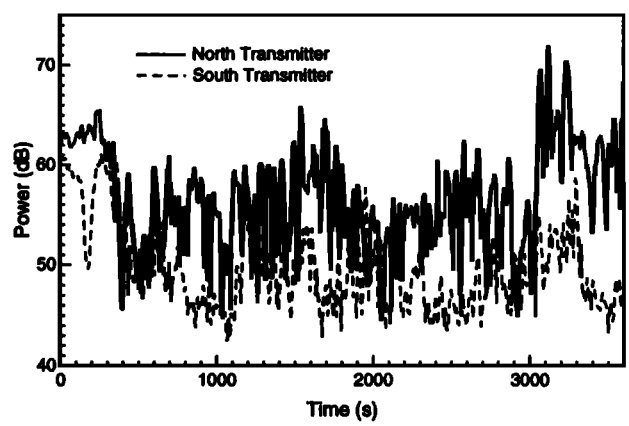

Figure 13. Total power received versus time after launch for the AA7 large barium release. Release occurred at 141 s. For this frequency (9.33 MHz) and for both paths (Guadeloupe North and South to Providenciales) there was a significant dropout that lasted nearly an hour.

Following the AA2 barium release (AA2) at 152 s after launch, the South Guadeloupe to Providenciales path at 11 MHz underwent a signal loss of at least 15 dB (Figure 14). Unfortunately, the receiver on that path experienced high internal noise, and we can only estimate that the signal dropped below the receiver noise level. It is also likely that the decrease in signal power at 1500 and 2000 s was caused by the Ba cloud. As shown in Figure 10, a second decrease in power was observed at 9.3 MHz for the Doppler peak near 0 Hz. The analogue of the peak with positive Doppler in Figure 10 did not appear at 11.3 MHz, so that Figure 14 represents the power only in the peak near 0 Hz which was likely the one-hop mode. A similar behavior was observed on the Guadeloupe to Grand Turk paths (Figure 15). On the basis of the appearance of the same behavior at multiple frequencies and different paths, we believe that both decreases in signal power were associated with the Ba release.

A brief period of multipath occurred at several frequencies lasting from 30 to 300 s following the AA4 depletion (Figure 16). Some of the four geographic paths at 11 MHz observed a large and sudden decrease in signal strength just before launch, which has made it difficult to quantify the effects of the release on these paths. We attribute the decrease to the loss of the *o* mode propagation caused by the decrease in maximum electron density in the *F* region. At approximately 500 s after launch the *x* mode was also lost; both modes were recovered later when the sunrise transition occurred. The most significant effect directly attributable to the depletion was an

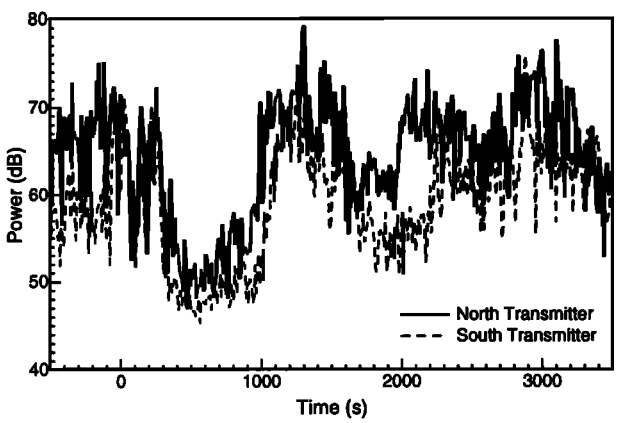

Figure 14. Total power received on the Guadeloupe to Providenciales path at 11.3 MHz for the AA2 barium release, which occurred at 152 s. Note in this data there are two large signal strength decreases that we believe were produced by the barium cloud.

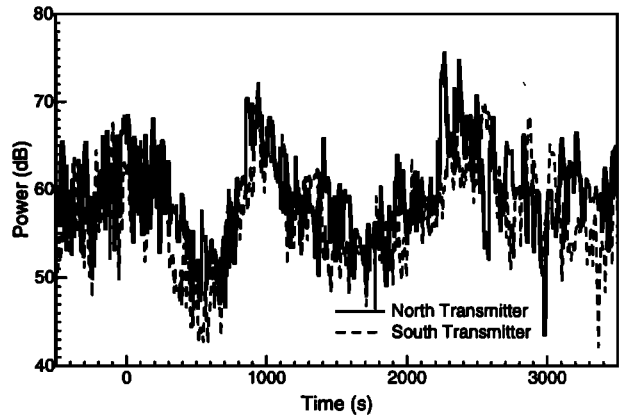

Figure 15. Similar to Figure 14, this shows the total power from Guadeloupe to Grand Turk at 11.3 MHz. Note that the general form of the data is similar but that the different paths do show somewhat different characteristics.

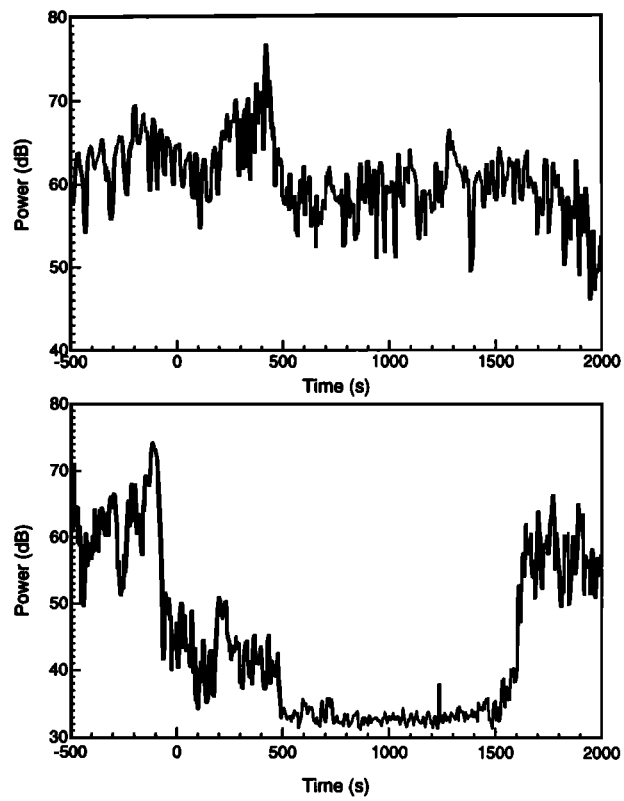

Figure 16. Total received power from the Coqui depletion experiment (AA4) for the Guadeloupe South to Grand Turk path at (top) 9 MHz and (bottom) 11 MHz. The strong decrease in signal strength at 11 MHz is due to a propagation effect and not the depletion.

increase in power of about 10 dB on the southern transmitter to Grand Turk at 9 MHz at about 400 s after launch (Figure 16). The increase indicates that the depletion caused a temporary focusing of the rays at this frequency.

4. Conclusions

We have studied the effects on HF propagation of ionospheric modifications produced by chemical releases during three experiments. The results of our CW measurements for the NICARE 1 depletion indicated that after an initial growth period of 100 to 200 s, new ray paths formed around the edges of the depletion [*Argo et al.*, 1992]. The NICARE 2 depletion showed similar early time behavior with a visible and extended chirp. No long-term behavior was detected because of the propagation geometry and the rapid filling of the depletion. The final set of experiments, Coqui, showed that propagation paths could be significantly disrupted by the release of chemicals at the proper location in the ionosphere.

For the depletions we found that there was an early chirp, with mostly negative Doppler shift and much lower power than the primary propagated path. Multipath produced by refraction by the depletion persisted for 10 min or more at some frequencies. The barium releases of the Coqui campaign caused significant signal reduction over a wide range of frequencies and paths. This was to be expected since the barium cloud acted as an opaque object blocking the propagation path and creating a shadow behind it.

Our data indicate that propagation or communication paths can be disrupted by moderate size chemical releases (tens of kilograms of material). The level of disruption was measured to be in the tens of decibels of signal strength degradation. For some communications systems this signal loss might create an inoperable condition.

Acknowledgments. This work was performed under the auspices of the U. S. Department of Energy by Los Alamos National Laboratory under contract W-7405-ENG-36. The authors thank the referees for their efforts in reviewing this paper.

References

Argo, P. E., T. Fitzgerald, and R. Carlos, NICARE 1 HF propagation experiment results and interpretation, *Radio Sci.*, *27*, 289–305, 1992.

Bernhardt, P. A., A critical comparison of ionospheric depletion chemicals, *J. Geophys. Res.*, *92*, 4617–4628, 1987.

Bernhardt, P. A., P. Rodriguez, C. L. Siefring, and C. S. Lin, Field-aligned dynamics of chemically induced perturbations to the ionosphere, *J. Geophys. Res.*, *96*, 13,887–13897, 1991.

Bernhardt, P. A., J. D. Huba, P. K. Chaturvedi, J. A. Fulford, P. A. Forsyth, D. N. Anderson, and S. T. Zalesak, Analysis of rocket beacon transmissions for computerized reconstruction of ionospheric densities, *Radio Sci.*, *28*, 613–627, 1993.

Bernhardt, P. A., et al., The ionospheric focused heating experiment, *J. Geophys. Res.*, *100*, 17,331–17,345, 1995.

Booker, H. G., A local reduction of F-region ionization due to missile transit, *J. Geophys. Res.*, *66*, 1073–1079, 1961.

Chang, N. J. F., Analysis of STRESS ionograms, *Tech. Rep. DNA 4486F*, SRI Int., Menlo Park, Calif., 1977.

Chesnut, W. G., G. N. Oetzel, and A. McKinley, A search by radar backscatter for irregularities produced by the Lagopedo F-region electron depletion releases, *Tech. Rep. DNA 4537F*, SRI Int., Menlo Park, Calif., 1978.

Djuth, F. T., El Coqui active experiments explore the ionosphere, *Soundings*, *2*, 1–3, 1993.

Djuth, F. T., M. P. Sulzer, J. H. Elder, and K. M. Groves, The CRRES AA2 release: HF wave-plasma interactions in a dense Ba+ cloud, *J. Geophys. Res.*, *100*, 17,347–17,366, 1995.

Kellogg, W. W., Pollution of the upper atmosphere by rockets, *Space Sci. Rev.*, *3*, 275–316, 1964.

Marmo, F. F., L. M. Aschenbrand, and J. Pressman, Artificial electron clouds, I, *Planet. Space Sci.*, *1*, 227–237, 1959.

Mendillo, M., Ionospheric holes: A review of theory and recent experiments, *Adv. Space Res.*, *8*, 1, 51–62, 1988.

Mendillo, M., and J. Forbes, Theory and observation of a dynamically evolving negative ion plasma, *J. Geophys. Res.*, *87*, 8273–8285, 1982.

Thome, G. D., Project SECEDE I HF radar studies of barium clouds, *Tech. Rep. RADC-TR-69-214*, Raytheon Co., Burlington, Mass., 1969.

Wagner, L. S., and J. A. Goldstein, Wideband hf channel probe: System description, *Tech. Rep. 8622*, Naval Res. Lab., Washington, D. C., 1983.

P. E. Argo, R. C. Carlos, T. J. Fitzgerald, Los Alamos National Laboratory, MS D466, Los Alamos, NM 87545.

(Received June 25, 1996; revised November 11, 1996; accepted November 21, 1996.)